



Published in final edited form as:

J Am Coll Cardiol. 2015 August 25; 66(8): 892–900. doi:10.1016/j.jacc.2015.06.1310.

Valve-Related Hemodynamics Mediate Human Bicuspid Aortopathy: Insights from Wall Shear Stress Mapping

David G. Guzzardi, BSc^{*}, Alex J. Barker, PhD[†], Pim van Ooij, PhD^{†,‡}, S. Chris Malaisrie, MD[§], Jyothy J. Puthumana, MD^{||}, Darrell D. Belke, PhD^{*}, Holly E.M. Mewhort, MD^{*}, Daniyil A. Svystonyuk, BSc^{*}, Sean Kang, BSc^{*}, Subodh Verma, MD, PhD^{||}, Jeremy Collins, MD[†], James Carr, MD[†], Robert O. Bonow, MD^{||}, Michael Markl, PhD^{†,‡}, James D. Thomas, MD^{||}, Patrick M. McCarthy, MD^{§,‡}, and Paul W.M. Fedak, MD, PhD^{*,§}

^{*}Department of Cardiac Sciences, Libin Cardiovascular Institute of Alberta, University of Calgary, Calgary, Canada [†]Department of Radiology, Feinberg School of Medicine, Northwestern University, Chicago, Illinois [‡]Department of Radiology, Academic Medical Center, Amsterdam, The Netherlands [§]Division of Surgery-Cardiac Surgery, Bluhm Cardiovascular Institute, Northwestern University, Chicago, Illinois ^{||}Department of Medicine-Cardiology, Bluhm Cardiovascular Institute, Northwestern University, Chicago, Illinois [¶]Division of Cardiac Surgery, Li Ka Shing Knowledge Institute of St. Michael's Hospital, University of Toronto, Toronto, Canada [#]Department of Biomedical Engineering, McCormick School of Engineering, Northwestern University, Chicago, Illinois

Abstract

BACKGROUND—Suspected genetic causes for extracellular matrix (ECM) dysregulation in the ascending aorta in patients with bicuspid aortic valves (BAV) has influenced strategies and thresholds for surgical resection of BAV aortopathy. Using 4-dimensional (4D) flow cardiac magnetic resonance imaging (CMR), we have documented increased regional wall shear stress (WSS) in the ascending aorta of BAV patients.

OBJECTIVES—We assessed the relationship between WSS and regional aortic tissue remodeling in BAV patients to determine the influence of regional WSS on the expression of ECM dysregulation.

METHODS—BAV patients (n = 20) undergoing ascending aortic resection underwent preoperative 4D flow CMR to regionally map WSS. Paired aortic wall samples (i.e., within-patient samples obtained from regions of elevated and normal WSS) were collected and compared for medial elastin degeneration by histology and ECM regulation by protein expression.

Corresponding Author: Paul W.M. Fedak, MD PhD, C880, 1403-29 Street NW, Calgary, Alberta, Canada, T2N 2T9, Telephone: (403) 944-5931, Fax: (403) 270-3715, paul.fedak@gmail.com.

Publisher's Disclaimer: This is a PDF file of an unedited manuscript that has been accepted for publication. As a service to our customers we are providing this early version of the manuscript. The manuscript will undergo copyediting, typesetting, and review of the resulting proof before it is published in its final citable form. Please note that during the production process errors may be discovered which could affect the content, and all legal disclaimers that apply to the journal pertain.

Disclosures: None.

RESULTS—Regions of increased WSS showed greater medial elastin degradation compared to adjacent areas with normal WSS: decreased total elastin ($p = 0.01$) with thinner fibers ($p = 0.00007$) that were farther apart ($p = 0.001$). Multiplex protein analyses of ECM regulatory molecules revealed an increase in transforming growth factor β -1 ($p = 0.04$), matrix metalloproteinase (MMP)-1 ($p = 0.03$), MMP-2 ($p = 0.06$), MMP-3 ($p = 0.02$), and tissue inhibitor of metalloproteinase-1 ($p = 0.04$) in elevated WSS regions, indicating ECM dysregulation in regions of high WSS.

CONCLUSIONS—Regions of increased WSS correspond with ECM dysregulation and elastic fiber degeneration in the ascending aorta of BAV patients, implicating valve-related hemodynamics as a contributing factor in the development of aortopathy. Further study to validate the use of 4D flow CMR as a noninvasive biomarker of disease progression and its ability to individualize resection strategies is warranted.

Keywords

aneurysm; imaging; remodeling

INTRODUCTION

Bicuspid aortic valves (BAVs) are associated with an increased predisposition towards dilation of the ascending aorta that could increase the rates of aortic complications such as aortic dissection, rupture, and/or sudden death (1,2). Although several dilation patterns have been proposed (2), considerable debate remains as to whether they are due to an inherent aortic wall defect (i.e., genetic aortopathy) or are secondary to valve-related changes in regional hemodynamics and shear stress (i.e., acquired etiology). A genetic etiology for BAV aortopathy is widely accepted and may prompt aggressive resection strategies to remove diseased tissues at risk of future complications (3,4). Increasingly, valve-related hemodynamics are believed to contribute to disease progression (5). Greater understanding of the pathophysiology of BAV aortopathy may facilitate improved surgical resection strategies, development of best practices and effective clinical guidelines, and in so doing, optimize clinical outcomes (6).

Flow sensitive cardiac magnetic resonance imaging (CMR) with full volumetric coverage of the ascending aorta (4-dimensional or 4D flow CMR) can measure and visualize complex aortic 3-dimensional (3D) blood flow patterns, such as flow jets, vortices, and helical flow. Using 4D flow CMR, we previously observed that normally functioning BAVs are associated with disturbed flow patterns in the ascending aorta with regional increases in wall shear stress (WSS) (7), a parameter known to be associated with vessel wall remodeling (8). We further established that the location of BAV cusp fusion is associated with different patterns of ascending aorta dilation (9). Recent studies have provided significant associative evidence that the pattern of cusp fusion corresponds with the expression of aortopathy (10,11), thus aligning with previous imaging findings implicating altered outflow patterns and the regional expression of elevated WSS with BAV morphology. To further investigate these findings, in this study we measured aortic WSS by 4D flow CMR in healthy normal volunteers and BAV patients to detect nonphysiological values and, for the first time,

correlated valve-related changes in WSS to regional tissue architecture and remodeling in paired BAV aortic wall tissue samples.

METHODS

With internal review board approval and informed consent, 20 BAV patients referred for ascending aortic surgery were enrolled. Patients with prior ascending aortic surgery or evidence of other forms of connective tissue disease were excluded. Healthy age-matched controls (n = 10) with tricuspid aortic valves were enrolled to compute regionally resolved 95% confidence interval (CI) values for physiologically normal aortic WSS (12); these controls had no evidence of cardiovascular disease and did not undergo surgery. The degree of aortic stenosis was graded based on absolute systolic peak velocity by continuous wave Doppler ultrasound (mild: 2 to 3 m/s; moderate/severe: ≥ 3 m/s) and aortic regurgitation was graded based on regurgitant fraction (mild: $<30\%$; moderate/severe: $\geq 30\%$) (13).

Participants received preoperative CMR at 1.5 T or 3 T (Magnetom Aera, Espree, Avanto, Skyra, Siemens Healthcare GmbH, Erlangen, Germany) to assess presence and significance of suspected BAV. 4D flow CMR provided complete volumetric coverage of the thoracic aorta for quantification of temporally resolved 3D blood flow velocities. Data were acquired during free breathing using respiratory and prospective electrocardiographic gating (14), with imaging parameters as described previously (12). Velocity encoding ranged from 150 to 400 cm/s based on the severity of valve stenosis. If glomerular filtration rate was >30 ml/min, gadopentetate dimeglumine, gadofosveset trisodium, or gadobenate dimeglumine were administered intravenously and flip angle was set to 15° ; otherwise, 7° was used. Patient-specific WSS heat maps of the BAV aorta were computed relative to a map of the population average for healthy age-matched controls as described in detail previously (12,15,16). WSS regions outside the healthy 95% CI were classified as abnormal. Intra-aortic regions of normal, depressed, and elevated WSS were mapped onto 3D visualizations of patient-specific aortas (**Figure 1**).

Aortic wall samples were collected as permitted by the extent of ascending aorta resection; surgeons were blinded to WSS heat maps. Samples were labeled according to preoperative zonal designations relative to the position of the right pulmonary artery (zones 1, 2, and 3 correspond to regions proximal, adjacent, and distal to the right pulmonary artery, respectively; **Figure 1**), and according to circumferential location (greater curvature, lesser curvature, anterior or posterior wall). Tissue samples were divided in 2 for histology and protein analysis, flash-frozen in optimal cutting temperature freezing compound (VWR International, Radnor, Pennsylvania) and liquid nitrogen within 15 min of resection and stored at -80° C until use. Paired samples of each patient's aorta from regions of normal and elevated WSS were compared.

Tissue designated for histology was thawed, sectioned circumferentially, and fixed in 10% buffered neutral formalin (VWR International) for a maximum of 1 week and paraffin-embedded. Sections of $6\ \mu\text{m}$ were mounted for Verhoeff-Van Gieson staining of medial elastin fibers. Chromatic analysis of elastin abundance was performed (Aperio ePathology, Leica Biosystems Inc., Buffalo Grove, Illinois). Total elastin content was computed as the

mean percent area of elastin staining relative to the total area analyzed of 6 representative fields of view (40X magnification) as selected by blinded observer. Distance between intact elastin fibers and their thicknesses were measured (ImageScope Viewing Software, Leica Biosystems Inc.) by blinded observer with a mean value computed for each sample taken from an average of 131 measurements per circumferentially sectioned slide (as described by Bauer and co-workers [17]).

Tissue designated for protein quantification was homogenized in 20 mM Tris-HCl buffer (pH 7.5, 0.5% Tween 20, 150 mM NaCl and Roche complete protease inhibitor 1:100) and centrifuged at $10,000 \times g$ for 10 min at 4°C. Supernatant containing 1.0 µg protein was assayed in duplicate for concentration of transforming growth factor β -1 (TGF β -1), matrix metalloproteinases (MMP), and tissue inhibitors of MMPs (TIMP) using the multiplex fluorescent bead assay (Eve Technologies, Calgary, Alberta, Canada).

STATISTICAL ANALYSIS

All group data are presented as mean \pm SD if normally distributed or as median (interquartile range [IQR] 25th quartile - 75th quartile) if non-normally distributed. Normality was assessed using the Shapiro-Wilk test. Normally and non-normally distributed data were compared using a paired Student *t* test or the Wilcoxon signed rank test, respectively (both 2-tailed). Cohort-averages between 2 groups were compared using Student *t* test when normally distributed or the Mann-Whitney test when non-normally distributed. Statistical analyses were performed using GraphPad Prism 6.0, with $p < 0.05$ considered statistically significant.

RESULTS

Patient demographics are summarized in **Table 1**. Healthy controls were used to define physiologically normal WSS values and were age-matched to BAV patients (50 ± 14 years vs. 48 ± 15 years respectively; $p = 0.83$). BAV patients were predominantly male with type 1 fusion of the right and left coronary cusps. Surgery was primarily indicated for BAV dysfunction; all patients had moderate/severe stenosis or regurgitation. Mean aortic diameter was 4.4 ± 0.5 cm at the sinus of Valsalva and 4.7 ± 0.6 cm for the ascending aorta. Most patients underwent aortic valve replacement (1 patient underwent BAV repair). All patients had ascending aortic resection with most requiring concomitant root replacement and a few undergoing hemi-arch resection using deep hypothermic circulatory arrest. Tissue corresponding to regions of normal and elevated WSS were primarily collected from zone 2 of the BAV aorta and from the anterior wall and greater curvature, respectively. Samples collected from patients are summarized in **Online Table 1**.

We quantified the total elastin content and architecture by histology image analysis. Aortic wall from regions of normal and elevated WSS demonstrated significantly decreased elastin content and architecture consistent with aortopathy (**Figures 1A through 1C**). Aortic wall exposed to elevated WSS showed reduced elastin abundance compared to aortic wall subjected to normal WSS within the same aorta ($p = 0.01$; **Figure 2A**). Similarly, the cohort-averaged percent area of elastin was significantly decreased in regions of elevated WSS

among BAV aortas ($36.61 \pm 16.87\%$ vs. $49.12 \pm 16.53\%$; $p = 0.04$; **Figure 2B**). Compared to aortic wall subjected to normal WSS, regions of elevated WSS had elastin fibers that were significantly thinner among patient pairs ($p = 0.00007$; **Figure 2C**). The absolute mean thickness of elastin fibers also was significantly decreased in regions of elevated WSS compared to regions of normal WSS ($2.72 \pm 0.40 \mu\text{m}$ vs. $3.25 \pm 0.27 \mu\text{m}$; $p = 0.00002$; **Figure 2D**). The median distance between elastin fibers was significantly greater in regions of elevated WSS compared to normal WSS ($p = 0.001$; **Figure 2E**). Similarly, cohort-averaged median distance between elastin fibers was significantly increased in aortic wall subjected to elevated WSS ($28.34 \mu\text{m}$ [IQR 22.03 -36.32] vs. $20.39 \mu\text{m}$ [IQR 18.35 - 24.43]; $p = 0.01$; **Figure 2F**).

Regions of elevated WSS had significantly higher concentrations of TGF β -1 protein ($p = 0.04$; **Figure 3**) compared to paired regions of normal WSS in the same aortas.

Aortic wall subjected to normal and elevated WSS within each patient's aorta were profiled for MMP and TIMP protein concentrations (**Table 2**). The absolute levels of MMP and TIMP protein expression in the samples were highly variable. MMP-2 and TIMP-2 were the most highly expressed MMP and TIMP in the aorta. Compared to regions of normal WSS, aortic wall exposed to elevated WSS demonstrated significantly increased relative concentrations of MMP-1 ($p = 0.03$), MMP-3 ($p = 0.02$), and TIMP-1 ($p = 0.04$), and there was a trend ($p = 0.06$) for increased concentrations of MMP-2.

DISCUSSION

BAV is an inheritable disorder and a genetic theory for the associated aortopathy is widely held, positing that the aorta has an inherent genetic weakness and is prone to dilation and rupture from an underlying dysregulation of extracellular matrix (ECM) in the aortic medial layer (1,5). This perspective has encouraged more aggressive approaches towards aortic resection using strategies similar to those applied in patients with proven genetic aortopathies, such as Marfan syndrome. Recently, we and others have shown that valve-related hemodynamics may play an important role in disease progression, where altered flow in the aorta is consistent with patterns of aortic dilation (9-11,18,19). Recognizing that hemodynamics may be altered in different regions of the ascending aorta, regional differences have been documented in key ECM proteins and cell phenotypic expressions, focused primarily on the convexity versus the concavity of the BAV aorta (20,21). These translational tissue studies suggest that valve-related hemodynamics may influence disease progression.

There is mounting evidence that both theories may coexist (5,22). Valve-related hemodynamics may exacerbate disease progression in genetically susceptible aortas (6). Given the absence of data showing a mechanistic link between cusp fusion patterns, altered aortic flow, and expression of disease, considerable debate surrounds the role of hemodynamics in mediating BAV aortopathy (5). Recently, using 4D flow CMR, we observed that even normally functioning BAVs are associated with disturbed ascending aortic flow and regional WSS increases, beyond the hemodynamic derangements accounted for by measures of stenosis and regurgitation (7). We further established that the location of

BAV cusp fusion was associated with different patterns of ascending aortic dilation (9), suggesting that valve-related hemodynamics may influence the expression of BAV aortopathy.

Despite well-documented changes of WSS in BAV patients, its role in the underlying aortopathy is unclear. In the current study, distinct regions of increased WSS were uniformly observed in BAV patients despite varied cusp fusion patterns and types or degrees of valve dysfunction. The significant relationship between WSS derived from 4D flow CMR and regional aortic tissue remodeling provides evidence, for the first time, of the role of valve-related hemodynamics in BAV aortopathy (**Central Illustration**).

WSS CORRESPONDS TO CHANGES RELATED TO AORTOPATHY

To validate the influence of regional WSS on tissue remodeling, we compared the medial matrix architecture between areas of high and normal WSS within each BAV aorta. This analysis is advantageous as each patient serves as his or her own control. Degeneration of the aortic media, particularly its elastic laminae, is the *sine qua non* of BAV aortopathy, with a hallmark of elastic fiber fragmentation (23). Bauer and colleagues also observed medial elastin degeneration characteristic of BAV aortopathy, documenting thinner elastic laminae and increased distances between laminae (17). In patients with BAV stenosis undergoing aortic valve replacement, Girdauskas and colleagues documented qualitative differences in aortic histology at the level of aortotomy with different systolic transvalvular flow patterns (24).

We observed disrupted medial elastin fiber architecture in the aortic wall of our patient cohort, consistent with BAV aortopathy, coupled with the novel finding that elastin fiber fragmentation and architectural derangement was significantly increased in areas of high versus normal WSS within the same aortas. Areas of normal WSS also had evidence of medial matrix degradation consistent with BAV aortopathy, although less severe than corresponding areas of high WSS. Given that histologic abnormalities are diffuse within the BAV aorta and our study population had relatively mild levels of aortic dilation (most <5.0 cm), the increased elastin degradation observed in the areas of high WSS relative to adjacent areas with normal WSS is a striking observation that provides strong evidence implicating valve-related hemodynamics in medial matrix degradation in BAV aortopathy.

TGF β is strongly implicated in the mechanotransduction of WSS upstream of flow-induced vascular remodeling (25). In animal models of human aortopathy, TGF β signaling is implicated in vascular disease and progression as a critical mediator of aortopathy (26). Forte and colleagues showed that TGF β and TGF β receptor-2 are increased in BAV aorta, suggesting a role for TGF β in mediating disease (20). In this study, we provide novel data linking aortic TGF β protein expression to local increases in WSS, with ascending aortic TGF β concentration significantly elevated in regions of high aortic WSS compared to adjacent regions with normal WSS. These data strongly implicate WSS as contributing to TGF β expression in the BAV aorta.

MMPs can directly degrade elastic ECM components. Supporting a mechanistic role for valve-related hemodynamics in MMP expression, Ikonomidis and colleagues showed altered

MMP profiles stratified by cusp fusion pattern in the BAV aorta (27). While many MMPs are expressed in the aorta, MMP-2 is highly implicated in aortic aneurysms and elastic matrix degeneration of remodeled arteries (28). Animal models provide proof of concept for WSS as a trigger for aortic wall MMP activation. For example, flow-mediated induction of MMP-2 expression was demonstrated in rabbit carotid arteries in association with medial matrix degeneration and vessel dilation (29). Furthermore, Atkins and colleagues modeled BAV-related elevated WSS in an ex vivo porcine aorta system, and found increased MMP-2 expression and activity (30). We previously reported evidence of MMP-2 elevations in the BAV aorta (31). The cumulative evidence by meta-analysis of all such studies confirms that MMP-2 is consistently elevated in human BAV aortopathy (32).

In the current study, we observed that aortic wall MMP-2 was the most highly expressed MMP in the BAV aorta, with a trend ($p = 0.06$) for greater expression in areas of high WSS as compared to adjacent areas with normal WSS in the same patients, and with significant increases in MMP-3 in the same areas. Importantly, the elevated levels of MMP-2, MMP-3, and TGF β areas of increased WSS were associated with fragmented medial elastin fibers. This observation also strongly implicates WSS in mediating BAV aortic disease progression. In addition to a direct role in degrading elastic tissue, it is noteworthy that MMP-2 and MMP-3 can activate latent TGF β and increase its activity. These factors may work synergistically to induce medial matrix remodeling.

The observed TIMP changes are complex and the substantial variability between patients and regions studied suggests that the regulatory control of TIMP expression is less influenced by WSS than specific MMPs and TGF β . TIMP-1 levels were increased in areas of high WSS but no significant difference was observed between groups with respect to other TIMP species. The lack of increased compensatory TIMP-2 expression in areas of high WSS may result in heightened MMP-2 activity. Further study is required to better define and understand the influence of specific MMPs and TIMPs in BAV aortopathy and their expression and activities with respect to valve-related hemodynamics.

STUDY LIMITATIONS

In our study, 4D flow CMR was used as a research tool to obtain WSS maps in individual patient aortas to better understand whether blood flow patterns play a role in the expression of BAV aortopathy. Given the spatial and temporal resolution of 4D flow CMR, underestimation of WSS is known to occur (7); however, relative WSS values (i.e., high/low WSS) are retained between subjects when consistent imaging parameters are employed. Here, we used similar parameters to those of a prior study that demonstrated the robustness of WSS measurements (33). Additionally, same-patient samples ensured that the relative WSS measurements were obtained in the same subject and same exam. Therefore, resolution was not deemed a significant factor for the study protocol to detect elevated WSS. While the concentrations of specific proteins of interest were examined, further studies should investigate TGF β and MMP-2 activities and other associated factors such as shifts in cell phenotype that may also mediate matrix remodeling. Additional comparison to patients with tricuspid valves and dilated aortas with areas of increased WSS should also be explored.

CONCLUSIONS

Regions of increased WSS correspond with ECM dysregulation and elastic fiber degeneration in the ascending aorta of BAV patients, implicating valve-related hemodynamics as a mediator of aortopathy. WSS as assessed by 4D flow CMR may serve as a noninvasive biomarker of regional aortic disease in patients with BAV aortopathy (deemed sufficiently severe to warrant operative intervention). Its utility in prediction of disease progression, particularly in earlier and less severe BAV aortopathy, awaits careful study, as does the efficacy of a targeted surgical approach incorporating regional aortic WSS.

Supplementary Material

Refer to Web version on PubMed Central for supplementary material.

Acknowledgments

The authors gratefully acknowledge the recruitment and organizational efforts of Colleen Clennon (Chicago), the staff of Northwestern's Center for Translational Imaging, Drs. Amy Bromley (Calgary) and Yong-Xiang Chen (Calgary) for their histological expertise, and Thomas Kryton for histological database management (Calgary).

Funding Sources: Melman Bicuspid Aortic Valve Program, Bluhm Cardiovascular Institute (PWMF), AHA 14POST20460151 (PvO), NIH K25HL119608 (AJB), and NIH R01HL115828 (MM).

ABBREVIATIONS AND ACRONYMS

4D flow CMR	time-resolved velocity-encoded phase contrast cardiac magnetic resonance imaging
BAV	bicuspid aortic valve
ECM	extracellular matrix
MMP	matrix metalloproteinase
TGFβ	transforming growth factor beta
TIMP	tissue inhibitor of MMP
WSS	wall shear stress

REFERENCES

1. Fedak PW, Verma S, David TE, et al. Clinical and pathophysiological implications of a bicuspid aortic valve. *Circulation*. 2002; 106:900–4. [PubMed: 12186790]
2. Verma S, Siu SC. Aortic dilatation in patients with bicuspid aortic valve. *N Engl J Med*. 2014; 370:1920–9. [PubMed: 24827036]
3. Verma S, Yanagawa B, Kalra S, et al. Knowledge, attitudes, and practice patterns in surgical management of bicuspid aortopathy: a survey of 100 cardiac surgeons. *J Thorac Cardiovasc Surg*. 2013; 146:1033–40. e4. [PubMed: 23988289]
4. Rinewalt D, McCarthy PM, Malaisrie SC, et al. Effect of aortic aneurysm replacement on outcomes after bicuspid aortic valve surgery: Validation of contemporary guidelines. *J Thorac Cardiovasc Surg*. 2014; 148:2060–9. [PubMed: 24755330]

5. Girdauskas E, Borger MA, Secknus MA, et al. Is aortopathy in bicuspid aortic valve disease a congenital defect or a result of abnormal hemodynamics? A critical reappraisal of a one-sided argument. *Eur J Cardiothorac Surg.* 2011; 39:809–14. [PubMed: 21342769]
6. Della Corte A, Body SC, Booher AM, et al. Surgical treatment of bicuspid aortic valve disease: knowledge gaps and research perspectives. *J Thorac Cardiovasc Surg.* 2014; 147:1749–57. 1757, e1. [PubMed: 24534676]
7. Barker AJ, Markl M, Burk J, et al. Bicuspid aortic valve is associated with altered wall shear stress in the ascending aorta. *Circ Cardiovasc Imaging.* 2012; 5:457–66. [PubMed: 22730420]
8. Lehoux S, Tedgui A. Cellular mechanics and gene expression in blood vessels. *J Biomech.* 2003; 36:631–43. [PubMed: 12694993]
9. Mahadevia R, Barker AJ, Schnell S, et al. Bicuspid aortic cusp fusion morphology alters aortic three-dimensional outflow patterns, wall shear stress, and expression of aortopathy. *Circulation.* 2014; 129:673–82. [PubMed: 24345403]
10. Kang JW, Song HG, Yang DH, et al. Association between bicuspid aortic valve phenotype and patterns of valvular dysfunction and bicuspid aortopathy: comprehensive evaluation using MDCT and echocardiography. *JACC Cardiovasc Imaging.* 2013; 6:150–61. [PubMed: 23489528]
11. Della Corte A, Bancone C, Dialecto G, et al. Towards an individualized approach to bicuspid aortopathy: different valve types have unique determinants of aortic dilatation. *Eur J Cardiothorac Surg.* 2014; 45:e118–24. discussion e124. [PubMed: 24420369]
12. van Ooij P, Potters WV, Collins J, et al. Characterization of Abnormal Wall Shear Stress Using 4D Flow MRI in Human Bicuspid Aortopathy. *Ann Biomed Eng.* 2015; 43(6):1385–97. [PubMed: 25118671]
13. Nishimura RA, Otto CM, Bonow RO, et al. 2014 AHA/ACC Guideline for the Management of Patients With Valvular Heart Disease: a report of the American College of Cardiology/American Heart Association Task Force on Practice Guidelines. *J Am Coll Cardiol.* 2014; 63:e57–185. [PubMed: 24603191]
14. Markl M, Harloff A, Bley TA, et al. Time-resolved 3D MR velocity mapping at 3T: improved navigator-gated assessment of vascular anatomy and blood flow. *J Magn Reson Imaging.* 2007; 25:824–31. [PubMed: 17345635]
15. van Ooij P, Potters WV, Nederveen AJ, et al. A methodology to detect abnormal relative wall shear stress on the full surface of the thoracic aorta using four-dimensional flow MRI. *Magn Reson Med.* 2015; 73:1216–27. [PubMed: 24753241]
16. Potters WV, van Ooij P, Marquering H, van Bavel E, Nederveen AJ. Volumetric arterial wall shear stress calculation based on cine contrast MRI. *J Magn Reson Imaging.* 2015; 41:505–16. [PubMed: 24436246]
17. Bauer M, Pasic M, Meyer R, et al. Morphometric analysis of aortic media in patients with bicuspid and tricuspid aortic valve. *Ann Thorac Surg.* 2002; 74:58–62. [PubMed: 12118804]
18. Bissell MM, Hess AT, Biasioli L, et al. Aortic dilation in bicuspid aortic valve disease: flow pattern is a major contributor and differs with valve fusion type. *Circ Cardiovasc Imaging.* 2013; 6:499–507. [PubMed: 23771987]
19. Hope MD, Hope TA, Meadows AK, et al. Bicuspid aortic valve: four-dimensional MR evaluation of ascending aortic systolic flow patterns. *Radiology.* 2010; 255:53–61. [PubMed: 20308444]
20. Forte A, Della Corte A, Grossi M, et al. Early cell changes and TGFbeta pathway alterations in the aortopathy associated with bicuspid aortic valve stenosis. *Clin Sci.* 2013; 124:97–108. [PubMed: 22857993]
21. Cotrufo M, Della Corte A, De Santo LS, et al. Different patterns of extracellular matrix protein expression in the convexity and the concavity of the dilated aorta with bicuspid aortic valve: preliminary results. *J Thorac Cardiovasc Surg.* 2005; 130:504–11. [PubMed: 16077420]
22. Della Corte A. The conundrum of aortic dissection in patients with bicuspid aortic valve: the tissue, the mechanics and the mathematics. *Q3 Eur J Cardiothorac Surg.* 2015; 48:150–1.
23. de Sa M, Moshkovitz Y, Butany J, David TE. Histologic abnormalities of the ascending aorta and pulmonary trunk in patients with bicuspid aortic valve disease: clinical relevance to the Ross procedure. *J Thorac Cardiovasc Surg.* 1999; 118:588–94. [PubMed: 10504620]

24. Girdauskas E, Rouman M, Disha K, et al. Correlation between systolic transvalvular flow and proximal aortic wall changes in bicuspid aortic valve stenosis. *Eur J Cardiothorac Surg.* 2014; 46:234–9. discussion 239. [PubMed: 24431167]
25. Ohno M, Cooke JP, Dzau VJ, Gibbons GH. Fluid shear stress induces endothelial transforming growth factor beta-1 transcription and production. Modulation by potassium channel blockade. *J Clin Invest.* 1995; 95:1363–9. [PubMed: 7883983]
26. Holm TM, Habashi JP, Doyle JJ, et al. Noncanonical TGFbeta signaling contributes to aortic aneurysm progression in Marfan syndrome mice. *Science.* 2011; 332:358–61. [PubMed: 21493862]
27. Ikonomidis JS, Ruddy JM, Benton SM Jr, et al. Aortic dilatation with bicuspid aortic valves: cusp fusion correlates to matrix metalloproteinases and inhibitors. *Ann Thorac Surg.* 2012; 93:457–63. [PubMed: 22206960]
28. Chung AW, Au Yeung K, Sandor GG, et al. Loss of elastic fiber integrity and reduction of vascular smooth muscle contraction resulting from the upregulated activities of matrix metalloproteinase-2 and -9 in the thoracic aortic aneurysm in Marfan syndrome. *Circ Res.* 2007; 101:512–22. [PubMed: 17641224]
29. Tronc F, Mallat Z, Lehoux S, et al. Role of matrix metalloproteinases in blood flow-induced arterial enlargement: interaction with NO. *Arterioscler Thromb Vasc Biol.* 2000; 20:E120–6. [PubMed: 11116076]
30. Atkins SK, Cao K, Rajamannan NM, Sucusky P. Bicuspid aortic valve hemodynamics induces abnormal medial remodeling in the convexity of porcine ascending aortas. *Biomech Model Mechan.* 2014; 13:1209–25.
31. Fedak PW, de Sa MP, Verma S, et al. Vascular matrix remodeling in patients with bicuspid aortic valve malformations: implications for aortic dilatation. *J Thorac Cardiovasc Surg.* 2003; 126:797–806. [PubMed: 14502156]
32. Rabkin SW. Differential expression of MMP-2, MMP-9 and TIMP proteins in thoracic aortic aneurysm - comparison with and without bicuspid aortic valve: a meta-analysis. *VASA Zeitschrift für Gefasskrankheiten.* 2014; 43:433–42. [PubMed: 25339161]
33. Markl M, Wallis W, Harloff A. Reproducibility of flow and wall shear stress analysis using flow-sensitive four-dimensional MRI. *J Magn Res Imaging.* 2011; 33:988–94.

PERSPECTIVES

COMPETENCY IN MEDICAL KNOWLEDGE: Measurements made using 4-dimensional magnetic resonance angiography (4-D flow MRI) suggest that valve-related hemodynamics contribute to the development of aortopathy in patients with bicuspid aortic valve (BAV).

TRANSLATIONAL OUTLOOK: Validation studies are needed to confirm the utility of 4D flow CMR as a noninvasive marker of disease progression, predictor of aortic dissection or rupture, and guide to the extent of surgical resection based on detailed measurements of regional aortic hemodynamics.

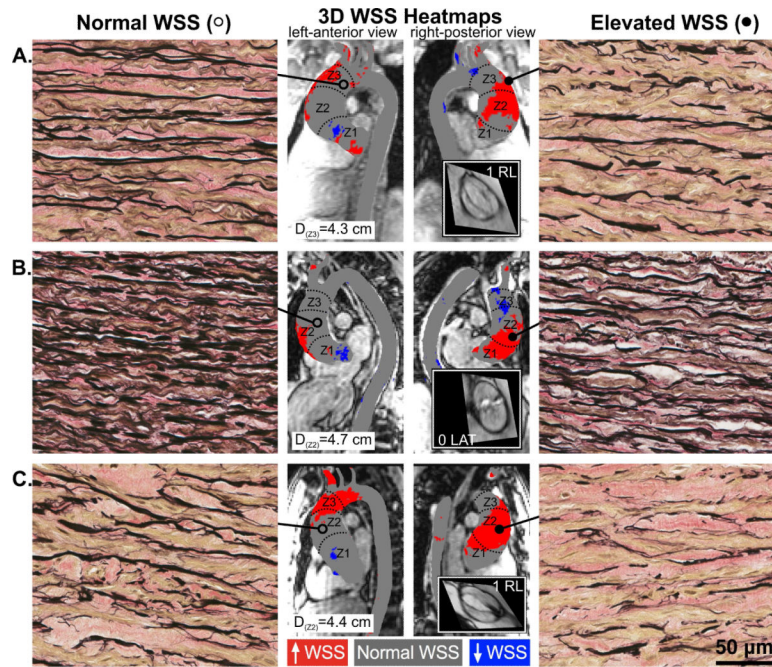


FIGURE 1. BAV Aortas: WSS Heat Maps and Elastin Fiber Staining

Aortic wall (A, B, and C denote 3 different bicuspid aortic valve [BAV] aortas) from regions of high wall shear stress (WSS) (right panels; closed circles) had fewer elastin fibers (black) that were thinner and farther apart compared to regions with normal WSS (left panels; open circles) in the same human aortas (40X magnification). Samples were collected from zones 1, 2, or 3, and from either the greater curvature, lesser curvature, anterior or posterior walls; accompanying diameters for tissue collection sites are shown. Grey denotes normal WSS within the 95% confidence interval compared to a healthy tricuspid aortic valve population; red and blue denote elevated and depressed WSS, respectively. Insets show steady-state free precession images of the aortic valve and Sievers valve phenotype. 3D = 3-dimensional.

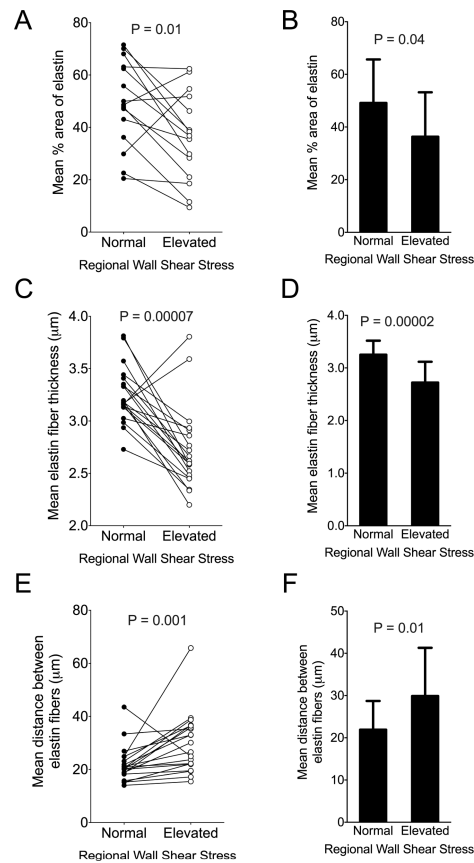


FIGURE 2. Metrics of Elastin Fiber Architecture

Elastin fiber characteristics from Verhoeff-Van Gieson elastin staining for patient pairs (**A**, **C**, **E**) and cumulative group means (**B**, **D**, **F**) for aortic wall subjected to normal and elevated WSS are shown. Total percent area of elastin staining was decreased in regions of elevated WSS compared to normal WSS (**A**, **B**), and remaining fibers were thinner (**C**, **D**). Greater distances between intact adjacent elastin fibers were observed in regions of elevated WSS (**E**, **F**). Abbreviations as in Figure 1.

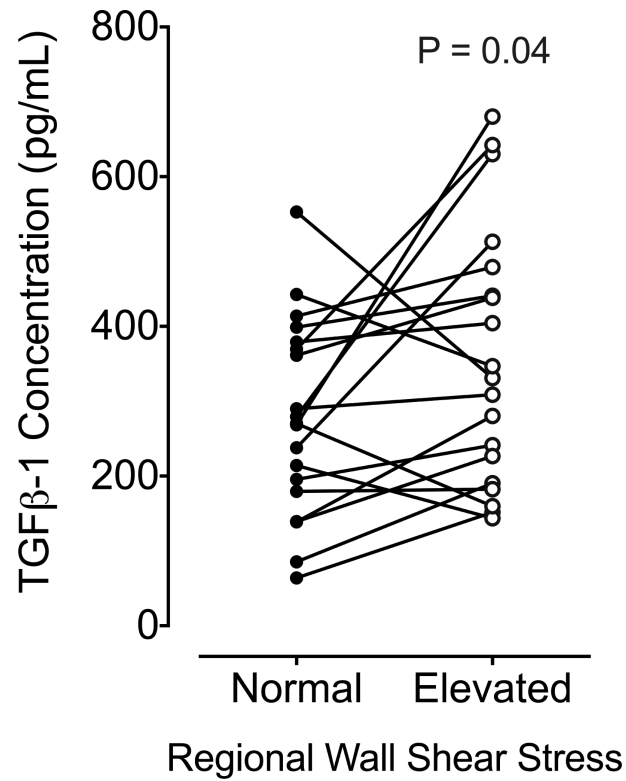
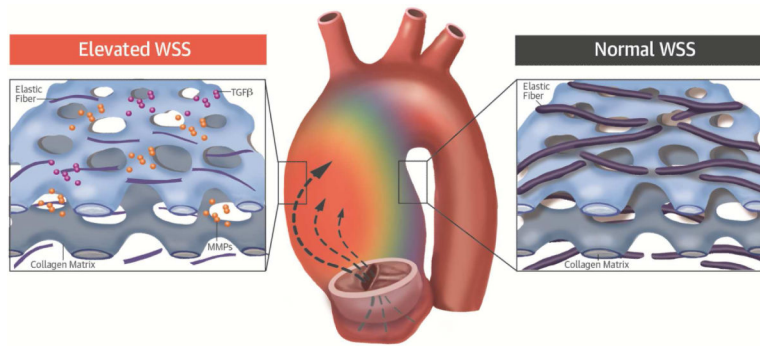


FIGURE 3. TGFβ-1 Concentrations in Regions of Normal and Elevated WSS

Absolute transforming growth factor beta (TGFβ-1) concentrations were greater in aortic wall regions of elevated compared to normal WSS. Solid lines denote group means, and p value represents analysis between paired patient samples (normal and elevated WSS).

Abbreviations as in Figure 1.



CENTRAL ILLUSTRATION. 4D Flow CMR and BAV Aortopathy

Using 4-dimensional flow cardiac magnetic resonance imaging (4D flow CMR), we assessed the relation between wall shear stress (WSS) and regional aortic tissue remodeling in bicuspid aortic valve (BAV) patients. Elevated aortic WSS generated by aberrant flow from cusp fusion corresponded to more severe extracellular matrix (ECM) dysregulation than adjacent regions of normal WSS in the same patient's aorta. Characteristic medial degeneration was observed throughout the aorta, but elastic fiber degeneration was more severe in regions of elevated WSS (less elastin, thinner fibers, and greater distances between laminae), where higher concentrations of mediators of ECM dysregulation (matrix metalloproteinase [MMP] and transforming growth factor beta [TGFβ]) are also observed. These data implicate valve-related hemodynamics as a contributing factor to BAV aortopathy.

TABLE 1

Patient Characteristics

Variable	BAV Study Population (N = 20)
Age, yrs	48 ± 15
Female	2 (10)
BAV classification	
Type 0, lateral	2 (10)
Type 1, RN	1 (5)
Type 1, RL	12 (60)
Type 2, RL/RN	5 (25)
Aortic diameter, cm	
Sinus of Valsalva	4.4 ± 0.5 (range: 3.7-5.7)
Mid ascending aorta	4.7 ± 0.6 (range: 3.6-6.3)
Aortic valve function	
No AS, moderate/severe AR	5 (25)
Mild AS, moderate/severe AR	1 (5)
Moderate/severe AS, no AR	5 (25)
Moderate/severe AS, mild AR	3 (15)
Moderate/severe AS, moderate/severe AR	6 (30)
Hypertension	7 (35)
Surgical procedure: aortic valve	
Repair	1 (5)
Replacement	19 (95)
AVR	4 (20)
Bentall	14 (70)
Ross	1 (5)
Surgical procedure: AsAo	
AsAo replacement	20 (100)
Root replacement	16 (80)
Hemi-arch	8 (40)

Values are mean ± SD or n (%).

AR = aortic regurgitation; AS = aortic stenosis; AsAo = ascending aorta; AVR = aortic valve replacement; BAV = bicuspid aortic valve; RN = right coronary-non-coronary cusp fusion; RL = right-left coronary cusp fusion.

TABLE 2

Absolute MMP and TIMP Concentrations in BAV Aortas

	Median Concentration (pg/ml)	IQR (pg/ml)	Range (pg/ml)	p Value
MMP-1*				
Elevated WSS	11.04	5.8-20.5	2.4-148.2	0.027
Normal WSS	8.84	3.5-14.7	1.3-19.3	
MMP-2				
Elevated WSS	8093.00	5062.0-13691.0	293.3-185897.0	0.064
Normal WSS	6060.00	2621.0-12910.0	197.1-119902.0	
MMP-3				
Elevated WSS	85.28	51.6-162.8	29.2-485.1	0.019
Normal WSS	58.46	43.4-115.9	6.8-363.8	
MMP-7*				
Elevated WSS	75.3 [†]	54.2 [‡]	8.5-165.6	0.653
Normal WSS	69.3 [†]	72.7 [‡]	0.0-235.3	
MMP-8				
Elevated WSS	2596.0	778.4-6258.0	22.4-22744.0	0.294
Normal WSS	3594.0	1754.0-7706.0	404.5-37267.0	
MMP-9				
Elevated WSS	4806.0	2377.0-19356.0	479.6-74046.0	0.596
Normal WSS	6581.0	3582.0-11796.0	1588.0-126759.0	
MMP-10*				
Elevated WSS	14.2	7.2-17.7	1.8-45.9	0.229
Normal WSS	10.5	8.1-13.1	0.7-36.1	
TIMP-1				
Elevated WSS	21442.0	11499.0-36679.0	4022.0-151540.0	0.040
Normal WSS	14546.0	8485.0-19629.0	4136.0-149919.0	
TIMP-2				
Elevated WSS	24931.0	15476.0-48537.0	10399.0-171363.0	0.756
Normal WSS	21721.0	14892.0-40513.0	6384.0-336986.0	
TIMP-3				
Elevated WSS	4138.0 [†]	2991.0 [‡]	0.0-11961.0	0.079
Normal WSS	3272.0 [†]	2794.0 [‡]	0.0-9862.0	
TIMP-4				
Elevated WSS	92.2	47.9-148.0	14.7-1173.0	0.165
Normal WSS	79.0	57.7-128.9	1.9-840.1	

Concentrations are reported as median [IQR] when non-normally distributed or mean ([†]) ± SD ([‡]) when normally distributed. P values denote paired analyses between regions of normal and elevated WSS in each BAV aorta.

IQR = interquartile range (25th quartile - 75th quartile); MMP = matrix metalloproteinase; TIMP = tissue inhibitor of MMP; WSS = wall shear stress; other abbreviations as in Table 1.

* Number of samples outside range of detection: MMP-1 = 7, MMP-7 = 10, MMP-10 = 2.